Available online at www.sciencedirect.com
ScienceDirect
Physica B 403 (2008) 2230–2234
PHYSICA B
www.elsevier.com/locate/physb

Raman scattering and luminescence study on arrays of ZnO doped with Tb^{3+}

Lei Yang[a,*], Yuanhong Tang[a,*], Aiping Hu[a], Xiaohua Chen[a], Kui Liang[a], Lide Zhang[b]

[a]College of Materials Science and Engineering, Hunan University, Changsha 410082, PR China
[b]Key Laboratory of Materials Physics, Institute of Solid State Physics, Chinese Academy of Sciences, P.O. Box 1129, Hefei 230031, PR China

Received 21 June 2007; received in revised form 3 December 2007; accepted 3 December 2007

Abstract

Ordered Tb^{3+}-doped zinc oxide nanowire arrays embedded in anodic alumina membranes (AAMs) were fabricated by an improved sol–gel method. They are hexagonal wurtzite structures with uniform diameter of about 30 nm. From the Raman spectra, the peak at about 439 cm^{-1} (E_2 (high) mode) decreases greatly, even disappears. It is seldom seen in ZnO. Compared with the undoped bulk ZnO, intensity of the peak at about 1005 cm^{-1} increases greatly and shifts towards the low Raman shift with the doping of Tb being increased. No luminescence of ZnO or Tb_2O_3 was found in luminescence spectra. They all indicated that Tb^{3+} ions did enter into the ZnO lattice.

Keywords: ZnO:Tb; Nanowire arrays; AMM; Raman

1. Introduction

Since the discovery of carbon nanotubes (CNTs) in 1991 [1], one-dimensional nanostructures such as wires, rods, belts, tubes, and whiskers have become the focus of intensive research, because of their potential applications in physical and chemical nanodevices [2–5]. ZnO is a wide-band-gap (3.37 eV) compound semiconductor with a large exciton binding energy (60 meV), which is considered as the most suitable material for UV devices when compared to the thermal energy (26 meV) of room temperature [6]. Furthermore, there are a number of potential applications of ZnO, such as transparent conducting films [7], surface acoustic devices (SAW) [8], sensors [9,10], solar cells [11], and so on. If rare-earth (RE) ions are incorporated into ZnO, its optical properties expected to be modified remarkably. For example, ZnO doped with Eu can emit red light and ZnO doped with Er or Tb can emit green light [12–14]. Among the RE elements, luminescence of Tb^{3+} is particularly interesting because the major emission band is near 544 nm, which is one of the three primary colors. However, it is difficult to incorporate RE ions effectively into ZnO nanocrystals using the chemical vapor deposition (CVD) method or the electrochemical deposition method, because of the high melting point of ZnO and RE_2O_3 and high standard electrode potential of RE. In this study, Tb^{3+}-doped ZnO nanowire arrays were prepared successfully by an improved sol–gel method using porous anodic alumina membranes (AAMs), and Raman scattering was studied [15,16]. Wurtzite zinc oxide is a hexagonal structure (space group C_{6V}^4) with lattice parameters, $a=0.3296$ nm and $c=0.5207$ nm. The unit cell contains two zinc cations and two oxygen anions. The ZnO crystal thus can be viewed as a sequence of O–Zn double layers stacked along the c-axis or (0 0 0 1) direction (Fig. 1). The tetrahedral coordination in ZnO results in a non-central symmetric structure and consequently in piezoelectricity and pyroelectricity.

2. Experimental

AAM used in this work was formed via anodization of aluminum metal in 0.3-M oxalic acidic solution, which had been studied in detail over the last five decades. Nitrate of Tb was prepared by dissolving terbium oxide in nitric acid,

*Corresponding authors. Tel.: +86 731 8821610; fax: +86 731 8821483.
E-mail addresses: yanglei@hnu.cn (L. Yang), yhtang@hnu.cn (Y. Tang).

0921-4526/$ - see front matter © 2008 Elsevier B.V. All rights reserved.
doi:10.1016/j.physb.2007.12.013

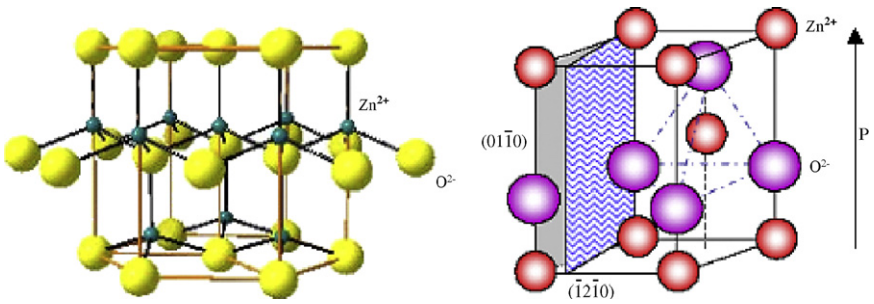

Fig. 1. The wurtzite structure model of ZnO. The bigger ion is O^{2-} and the smaller ion is Zn^{2+}.

and addition of several drops of H_2O_2 was necessary in the dissolving process. Ethylene glycol and urea used in this experiment were of A.R. grade. In the experiment, 0.3 g of $Zn(NO_3)_2 \cdot 6H_2O$ was dissolved into 100 mL deionized water to form a 0.01-M aqueous solution. Nitrate of Tb was added into the solution. The molar ratio of Tb to Zn was 2.5%, 5%, 7.5%, 10%, and 12.5% each. The pH value of the solution was adjusted to near neutral using aqueous ammonia and dilute nitric acid. Then 0.3 g of urea and 5 mL of ethylene glycol were added into the solution. The AAM was placed in a beaker that contained the above-mentioned mixed solution, and then the beaker was sealed with an adhesive tape. Subsequently, the beaker was maintained at 60 °C for 48 h and then at 80 °C for 48 h. Finally, the AAM was taken out, washed repeatedly, and then placed in a muffle furnace kept at 700 °C for 10 h. The morphology of the as-synthesized sample was obtained with transmission electron microscopy (TEM JEM-2021) and scanning electron microscopy (FE-SEM Sirion 200). Raman scattering measurements were performed using a LABRAM-HR Raman microspectroscopy.

3. Results and discussions

Five XRD patterns of the as-prepared samples doped with the molar ratio of Tb to Zn of 2.5%, 5%, 7.5%, 10%, and 12.5%, respectively, are shown in Fig. 2. The diffraction peaks can be indexed to a hexagonal wurtzite structure of ZnO. Compared with JCPDS data, all the diffraction peaks are shifted slightly towards the low diffraction angle indicating that the lattice parameters of Tb-doped ZnO are a little larger than those of undoped ZnO. No XRD peaks related to Tb compounds were found. So it is suggested that Tb^{3+} ions occupy Zn sites or interstitial sites in the ZnO lattice.

The morphology of the as-synthesized sample was obtained with FE-SEM and TEM. Fig. 3a displays the top view SEM image of the ZnO:Tb nanowire arrays grown within an AAM. The TEM images of the product are shown in Fig. 3b. The inset of Fig. 3b presents the selected area electron diffraction (SAED) pattern taken from the single nanowire. It can be observed that large-scale polycrystals were produced with a uniform diameter

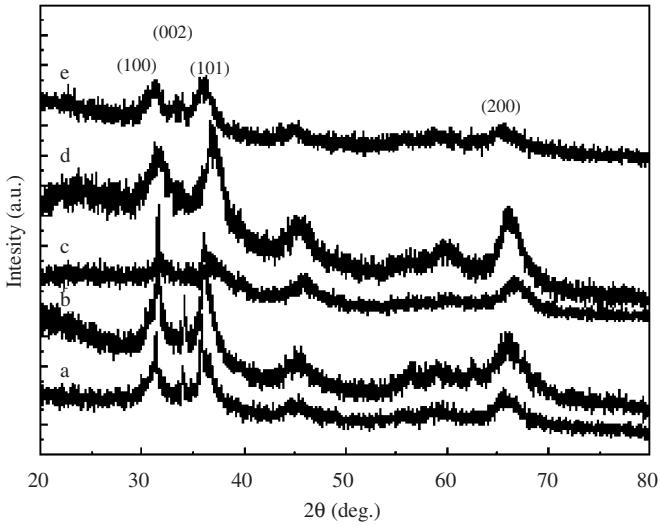

Fig. 2. The XRD diffraction patterns of ZnO:Tb nanowire arrays. The molar ratio of Tb to Zn: (a) 2.5%, (b) 5%, (c) 7.5%, (d) 10%, and (e) 12.5%.

of about 30 nm. The micrograph shows that the ZnO:Tb nanowires are roughly parallel to each other, and vertical to the AMM surface. It is found that almost all the pores in AMM are filled with ZnO:Tb nanowires.

Fig. 4 shows the room-temperature Raman spectra of the ZnO:Tb nanowires array with the molar ratio of Tb to Zn of 2.5%, 5%, 7.5%, 10%, and 12.5%, respectively. The curve *f* is the Raman spectrum for the undoped standard bulk ZnO. Since the hexagonal wurtzite structure of ZnO belongs to the space group C_{6V}^4 (P63mc), one primitive cell includes two formula units, with all of the atoms occupying 2b sites of symmetry C_{3V}. Group theory predicts the existence of the following optic modes: $A_1 + 2B_1 + E_1 + 2E_2$ at the Γ point of the Brillouin zone; B_1 (low) and B_1 (high) modes are normally silent; A_1, E_1, and E_2 modes are Raman-active; and A_1 and E_1 also are infrared-active. Thus, A_1 and E_1 are split into longitudinal (LO) and transverse (TO) optical components. In the curve *f*, the peaks at 329 and 660 cm^{-1} are A_1 symmetry modes, the peak at 437 cm^{-1} is attributed to ZnO non-polar optical phonons high E_2 mode, while the peak at 378 cm^{-1} corresponds to A_1 symmetry with the TO mode. The peaks at 583 and 1156 cm^{-1} are E_1 symmetry with LO and

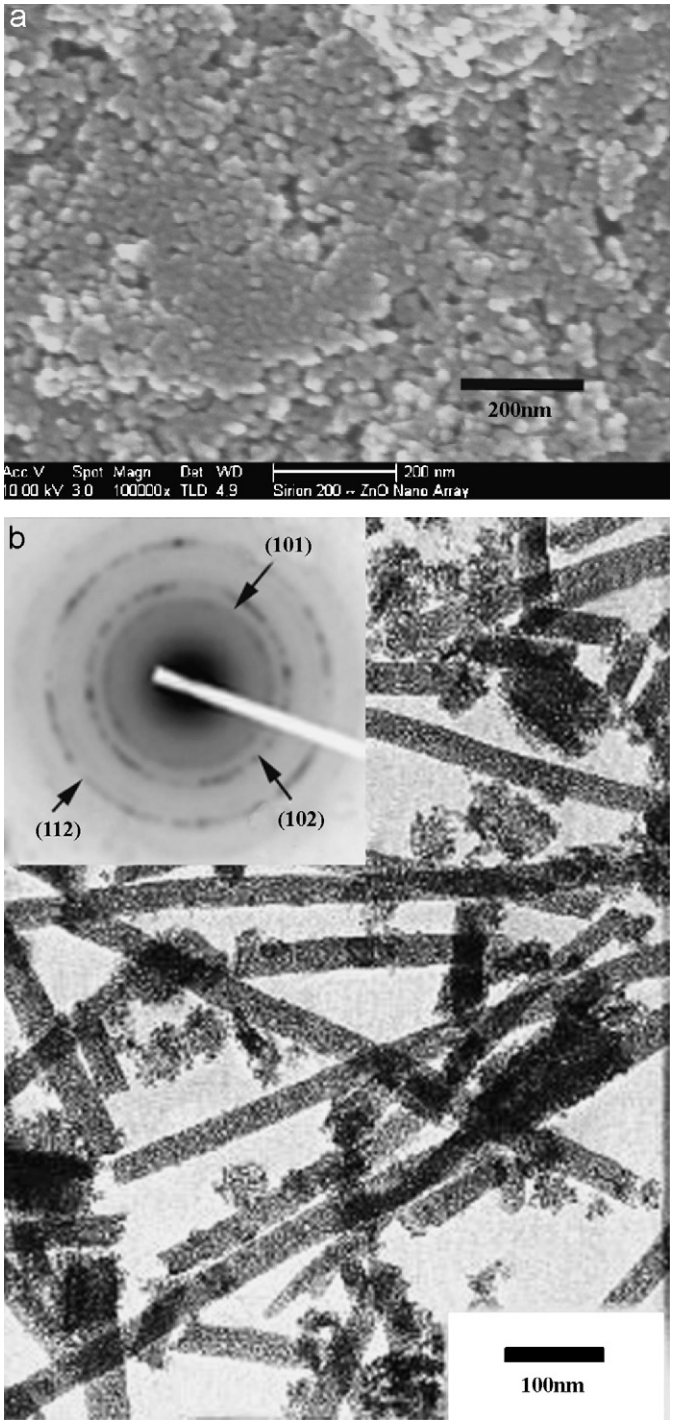

Fig. 3. The SEM and TEM images of ZnO:Tb nanowire arrays: (a) typical SEM image of ZnO:Tb nanowire arrays and (b) typical TEM image of the ZnO:Tb nanowires and its selected area electron diffraction.

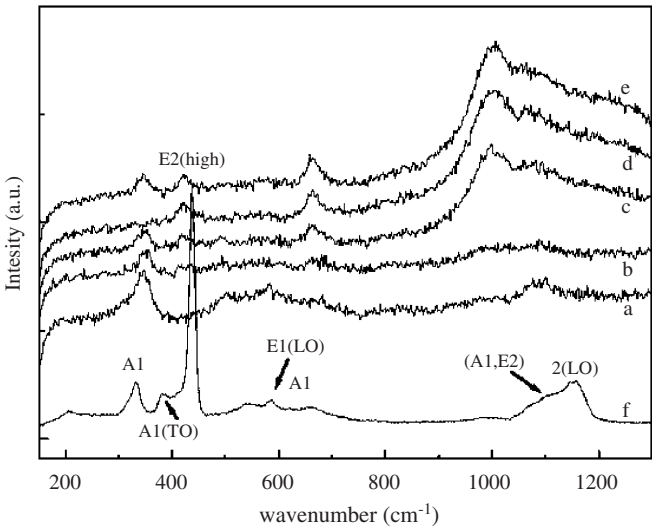

Fig. 4. The Raman spectra of ZnO:Tb nanowire arrays. The molar ratio of Tb to Zn: (a) 2.5%, (b) 5%, (c) 7.5%, (d) 10%, and (e) 12.5%. Curve *f* is undoped bulk ZnO.

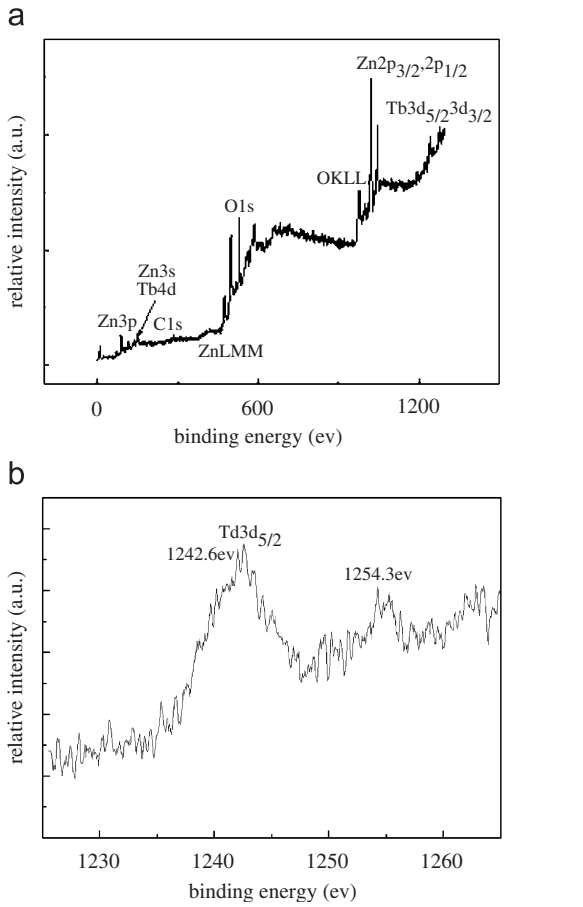

Fig. 5. XPS of the sample. (a) XPS of the sample doped with the molar ratio of Tb to Zn = 10% and (b) $Tb3d_{5/2}$ core-level X-ray photoelectron spectra of ZnO:Tb nanowires arrays.

2LO modes, respectively. The peak at 1101 cm^{-1} is A_1, E_2 (Acoust. comb) symmetry mode.

In Fig. 4, Raman curve of ZnO:Tb is almost the same as the bulk ZnO materials. So the main structure of ZnO is not changed after being doped with Tb. When the size of the particles reduces to nanoscale, the $k = 0$ selection rule for the first-order Raman scattering is relaxed, and the phonon scattering will not be limited to the center of the Brillouin zone; hence, the phonon dispersion near the center of the Brillouin zone should be considered as well.

As a result, the shift and broadening of the first-order optical phonon scattering modes will be observed [17,18]. In Fig. 3, the intensity of E_1 (2LO) mode of the ZnO:Tb nanowire arrays was increased greatly and shifted towards the low Raman shift compared with the bulk sample. It indicates that the size of the ZnO:Tb nanowire is at nanograde. It is also confirmed by TEM images. Compared with the undoped bulk ZnO material, when ZnO is doped with Tb^{3+} the Raman peak at about 439 cm^{-1} (E_2 (high) mode) decreases greatly, even disappears. The same phenomenon occurred in the system of ZnO doped with another RE element: Ce [19]. It indicates that after being doped with Tb^{3+}, the ZnO lattice is malformed with the result that the E_2 (high) mode decreases greatly.

Further evidence for the composition was obtained by the XPS. Fig. 5a is a survey spectrum and Fig. 5b shows XPS spectrum taken from the $Tb3d_{5/2}$ regions of the ZnO:Tb nanowires array. In Fig. 5a, there are two peaks at about 1242 and 1277 eV, which are attributed to photoemission peaks from $Tb3d_{5/2}$ and $Tb3d_{3/2}$. $Zn2p_{3/2}$, $Zn2p_{1/2}$ and O1s are also found. The atomic composition of Tb, Zn, and O was calculated by using the integrated peak area and sensitivity factors, and the atomic ratio of Tb:Zn:O is about 0.1:1:1. In Fig. 5b there are two peaks at 1242.6 and 1254.3 eV, which are attributed to photoemission peaks from $Tb3d_{5/2}$ and energy loss structure, respectively. Compared with the standard peak of $Tb3d_{5/2}$ (1241.2 eV) in Tb_2O_3, there is a blue-shift in the spectrum indicating that the distance of Tb to O in the ZnO:Tb crystal is different from the distance of Tb to O in the Tb_2O_3 oxide. It indicates that Tb^{3+} ions occupy the Zn sites or interstitial sites in the ZnO lattice.

The luminescence spectra of five samples at room temperature are shown in Fig. 6. The emission spectra for ZnO:Tb consist of four main lines at 488 nm ($^5D_4 \rightarrow {}^7F_6$), 543 nm ($^5D_4 \rightarrow {}^7F_5$), 586 nm ($^5D_4 \rightarrow {}^7F_4$), and 622 nm ($^5D_4 \rightarrow {}^7F_3$) under 377 nm excitation, which correspond to electric dipole transitions of the Tb^{3+} ions, and the electronic transition, $^5D_4 \rightarrow {}^7F_5$, is the strongest [20,21]. No luminescence of ZnO or Tb_2O_3 was found. It indicates that Tb^{3+} ions enter into the ZnO lattice; they may occupy the Zn sites or interstitial sites in the ZnO lattice. The ionic radius of Tb^{3+} is 0.092 nm and the ionic radius of Zn^{2+} is 0.074 nm. So Tb^{3+} may occupy the Zn sites, because the ionic radius of Tb^{3+} is little bigger than that of Zn^{2+}. Zn^{2+} is bivalent and Tb^{3+} is trivalent. So it is believed that when Tb^{3+} occupied the Zn sites, the probability of the neighboring Zn^{2+} being vacant is a half. From Fig. 6, it can be seen that the peak of ZnO doped with 10% of Tb^{3+} is highest and ZnO doped with 12.5% of Tb is weak, because of the quench effect.

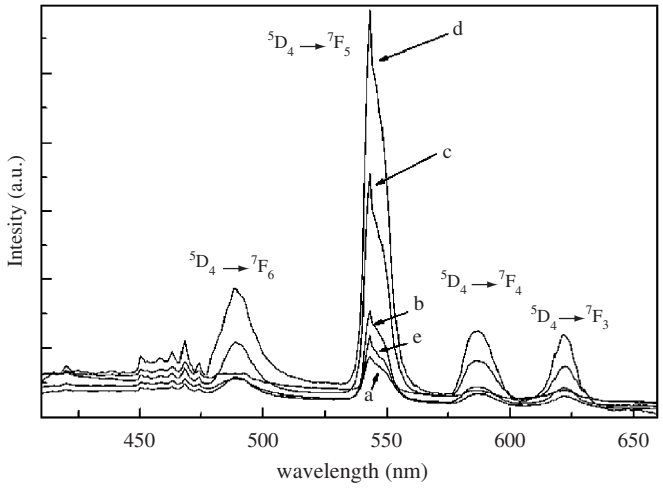

Fig. 6. The emission spectra of ZnO:Tb nanowire arrays. The molar ratio of Tb to Zn: (a) 2.5%, (b) 5%, (c) 7.5%, (d) 10%, and (e) 12.5%.

4. Conclusions

Ordered Tb^{3+}-doped zinc oxide nanowire arrays embedded in AAMs were fabricated by an improved sol–gel method. The nanowires with the uniform diameter of about 30 nm are hexagonal wurtzite structures. From the Raman spectrum, compared with undoped bulk ZnO, the peak at about 439 cm^{-1} (E_2 (high) mode) decreases greatly and even disappears, and the intensity of the peak at about 1005 cm^{-1} increases greatly and shifts towards the low Raman shift with the doping of Tb being increased. No luminescence of ZnO or Tb_2O_3 was found in luminescence spectra. They all indicated that Tb^{3+} ions did enter into the ZnO lattice, and Tb^{3+} may occupy the Zn sites in all probability.

Acknowledgments

This work was supported by the Ministry of Science and Technology of China (Grant no. 1999064501) and the Ministry of Education of China (Grant no. 2004532014 and no. 20080548076).

References

[1] N.P. Balsara, S. Ijima, Nature 354 (1991) 56.
[2] Z.W. Pan, Z.R. Dai, Z.L. Wang, Science 291 (2001) 1947.
[3] L.D. Zhang, G.W. Meng, F. Phillipp, Mater. Sci. Eng. A 286 (2000) 34.
[4] G.S. Chen, S.H. Chen, X.G. Zhu, Y.O. Mao, L.D. Zhang, Mater. Sci. Eng. A 286 (2000) 165.
[5] D.W. Wang, A.J. Millis, S.D. Sarma, Phys. Rev. Lett. 85 (2000) 4570.
[6] Y.R. Ryua, S. Zhub, J.D. Budai, J. Appl. Phys. 88 (2000) 201.
[7] M. Chen, Z.L. Pei, X. Wang, C. Sun, L.S. Wen, J. Vac. Sci. Technol. A 19 (2001) 963.
[8] C.R. Gorla, N.W. Emanetoglu, S. Liang, W.E. Mayo, Y. Lu, J. Appl. Phys. 85 (1999) 2595.
[9] S.C. Minne, S.R. Manalis, C.F. Quate, Appl. Phys. Lett. 67 (1999) 3918.
[10] J.F. Chang, H.H. Kuo, I.C. Leu, M.H. Hon, Sensors Actuators B: Chem. 84 (2002) 258.
[11] H. Rensmo, K. Keis, J. Phys. Chem. B 101 (1997) 2598.
[12] Y.K. Park, J.I. Han, M.G. Kwak, Appl. Phys. Lett. 72 (1998) 668.
[13] M. Kohls, M. Bonanni, L. Spanhel, D. Su, M. Giersig, Appl. Phys. Lett. 81 (2002) 3858.

[14] S.M. Liu, F.Q. Liu, H.Q. Guo, Z.H. Zhang, Z.G. Wang, Phys. Lett. A 271 (2000) 128.
[15] G.S. Wu, L.D. Zhang, B.C. Cheng, T. Xie, X.Y. Yuan, J. Am. Chem. Soc. 126 (2004) 5976.
[16] L. Yang, Y. Li, Y.H. Xiao, C.H. Ye, L.D. Zhang, Chem. Lett. 34 (2005) 828.
[17] G. Scamarcio, V. Spagnolo, G. Ventruti, M. Lugara, G.C. Righini, Phys. Rev. B 53 (1996) 10489.
[18] B.C. Cheng, Y.H. Xiao, G.S. Wu, L.D. Zhang, Appl. Phys. Lett. 84 (2004) 416.
[19] M.C. Klein, F. Hache, D. Ricard, C. Flyzanis, Phys. Rev. B 42 (1990) 11123.
[20] G.R. Jeff, E.S. Gregory, B. Gordon, R.S. Paul, J. Phys. Chem. B 107 (2003) 12862.
[21] G. Jones II, I. Valentine, Photochem. Photobiol. Sci. 1 (2002) 925.